

Alkali Metal Ions Insertion/Extraction Reactions with Hollandite-Type Manganese Oxide in the Aqueous Phase

Qi Feng,* Hirofumi Kanoh, Yoshitaka Miyai, and Kenta Ooi

Shikoku National Industrial Research Institute,
2217-14-hayashi-cho Takamatsu-shi Kagawa 761-03, Japan

Received July 8, 1994. Revised Manuscript Received November 9, 1994[⊗]

H⁺-form hollandite-type manganese oxide (HolMO) was prepared directly by reacting LiMnO₄ with Mn²⁺ in H₂SO₄ solution. The insertion/extraction reactions of alkali metal ions with HolMO were investigated by chemical, X-ray, DTA-TG analyses, FT-IR spectroscopy, pH titration, and K_d measurements. The alkali metal ions were inserted/extracted by two different mechanisms: redox-type and ion-exchange-type reactions. A model for the insertion/extraction reactions was proposed. The hollandite-type manganese oxide showed an ion-sieve property (the effective pore radius of the ion sieve is 1.41 Å) for the adsorption of alkali and alkaline earth metal ions.

Introduction

Hollandite- or cryptomelane-type manganese oxides have a one-dimensional (2 × 2) tunnel structure, as shown in Figure 1. K⁺, NH₄⁺, Na⁺, and Ba²⁺ ions generally occupy the (2 × 2) tunnel sites.¹⁻⁴ The hollandite-type manganese oxides show cation-adsorptive properties in the aqueous phase after extraction of the metal cations in the tunnel sites.⁵⁻⁸ The electrochemical studies from a standpoint of developing non-aqueous lithium batteries have indicated that Li⁺ can be extracted/inserted topotactically from/into the hollandite-type manganese oxides in the organic phase, and the manganese oxides can be used as a cathode material for lithium batteries.^{3,9,10}

Tsuji et al. have studied the ion-exchange mechanism on a hollandite-type (cryptomelane-type) manganese oxide with K⁺ in the (2 × 2) tunnel sites in the aqueous phase.¹¹⁻¹³ The K⁺ can be topotactically extracted by treating with a concentrated HNO₃ (13 M). The K⁺-extracted manganese oxide (CryMO) shows specifically high selectivity for the adsorptions of K⁺, Rb⁺, Ba²⁺, and Pb²⁺ among alkali, alkaline earth, and transition-metal ions. The selective properties can be explained by the ion-sieve effect of the (2 × 2) tunnel which has a suitable size for fixing ions having an effective ionic radius of

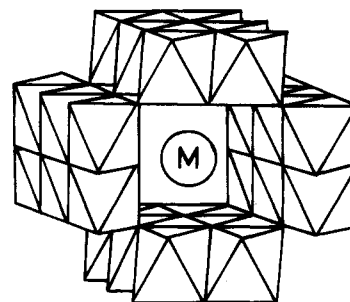
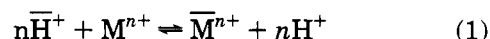
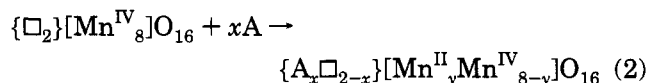


Figure 1. Structure of hollandite-type manganese oxide. The MnO₆ octahedra link together, sharing edges to form the (2 × 2) tunnel structure.

about 1.4 Å. An H⁺/Mⁿ⁺ ion-exchange reaction (eq 1) has been proposed for the adsorption of metal ions,¹¹



where \bar{H}^+ denotes an exchangeable proton in the solid phase. On the other hand, a redox-type reaction has been proposed also for the adsorption of metal ions by other studies.¹⁴⁻¹⁶ The reaction can be represented by the following equation:



where { } denotes (2 × 2) tunnel sites, [] octahedral sites occupied by manganese, □ vacant structural sites, and A is a metal ion and possibly also NH₄⁺.

We have studied the mechanism of Li⁺ extraction/insertion reactions with spinel-type manganese oxides in the aqueous phase.¹⁷⁻¹⁹ Li⁺ can be extracted/inserted topotactically from/into the spinel-type manganese oxides by two types of reactions: redox-type and ion-exchange type. The Li⁺ extraction/insertion sites can

[⊗] Abstract published in *Advance ACS Abstracts*, December 15, 1994.

(1) Burns, R. G.; Burns, V. M. *Manganese Dioxide Symposium*; Tokyo, 1980; Vol. 2, p 97.

(2) Bystrom, A.; Bystrom, A. M. *Acta Crystallogr.* **1950**, *3*, 146.

(3) Ohzuku, T.; Kitagawa, M.; Sawai, K.; Hirai, T. *J. Electrochem. Soc.* **1991**, *138*, 360.

(4) Fernandes, J. B.; Desai, B.; Dalal, V. N. K. *Electrochim. Acta* **1983**, *28*, 309.

(5) Ooi, K.; Miyai, Y.; Katoh, S. *Sep. Sci. Technol.* **1987**, *22*, 1779.

(6) Gruner, J. W. *Am. Mineral.* **1943**, *28*, 497.

(7) Tsuji, M.; Tanaka, Y.; Abe, M.; Tanaka, Y. *New Development in Ion Exchange*; Tokyo, 1991; p 627.

(8) Tsuji, M.; Abe, M.; Tanaka, Y.; Tanaka, Y. *Seventh Symposium on Salt*; 1993; Vol. II, p 23.

(9) Rossouw, M. H.; Liles, D. C.; Thackeray, M. M.; David, W. I. F.; Hull, S. *Mater. Res. Bull.* **1992**, *27*, 221.

(10) Feng, Q.; Kanoh, H.; Ooi, K.; Tani, M.; Nakacho, Y. *J. Electrochem. Soc.* **1994**, *141*, L135.

(11) Tsuji, M.; Abe, M. *Solvent Extr. Ion Exch.* **1984**, *2*, 253.

(12) Tsuji, M.; Abe, M. *Bull. Chem. Soc. Jpn.* **1985**, *58*, 1109.

(13) Tsuji, M.; Komarneni, S. *J. mater. Res.* **1993**, *8*, 611.

(14) Mathieson, A. M.; Wadsley, A. D. *Am. Mineral.* **1950**, *35*, 99.

(15) Butler, G.; Thirsk, H. R. *Acta Crystallogr.* **1952**, *5*, 288.

(16) Feitknecht, W.; Buser, W. *Z. Elektrochem.* **1956**, *45*, 871.

(17) Feng, Q.; Miyai, Y.; Kanoh, H.; Ooi, K. *Langmuir* **1992**, *8*, 1861.

(18) Feng, Q.; Miyai, Y.; Kanoh, H.; Ooi, K. *Chem. Mater.* **1993**, *5*, 311.

(19) Ooi, K.; Miyai, Y.; Sakakihara, J. *Langmuir* **1991**, *7*, 1167.

be classified into redox-type and ion-exchange-type sites. The number of redox-type and ion-exchange-type sites correlates well with the amount of trivalent Mn ions and the defects of the Mn ions in the lithium-manganese oxide spinels, respectively.¹⁷ These two types of sites mix with each other and form a one-phase solid solution system.

We think metal ions can be inserted/extracted also into/from the hollandite-type manganese oxide by both redox-type and ion-exchange-type reactions, similar to the case of the spinel-type manganese oxide, because manganese oxides have the characteristics of both easy conversion between Mn(III) and Mn(IV) and formation defects in the crystals. The present paper describes a fundamental study of alkali metal ions insertion/extraction reactions with hollandite-type manganese oxide (HolMO) prepared directly by reacting LiMnO_4 with Mn^{2+} in H_2SO_4 solution.¹⁰ Since HolMO contains only a small amount of Li^+ in the (2×2) tunnel sites, it matches the purpose of the present study.

Experimental Section

Materials. Hollandite-type manganese oxide (HolMO) was prepared by the method described in a preceding paper.¹⁰ A 0.2 M LiMnO_4 solution (100 mL) was poured into a 0.3 M $\text{Mn}(\text{NO}_3)_2$ solution (100 mL) containing 8 M H_2SO_4 at 100 °C with stirring. After reacting for 2 h, the mixed solution was kept at 60 °C for 1 day. The product was filtered, washed with water, and air-dried at 70 °C for 1 day. The sample was designated as HolMO.

Alkali Metal Ions Insertion/Extraction Reactions. Li^+ , K^+ , and Cs^+ insertion and extraction reactions with HolMO were investigated at room temperature. In the insertion study, HolMO (2 g) was immersed in a 1 M MOH ($M = \text{Li}, \text{K}, \text{or Cs}$) solution (200 mL) for 7 days to obtain the alkali metal ions inserted samples (HolMO(Li), HolMO(K), or HolMO(Cs)), respectively. In the extraction study, 0.5 g of the inserted sample (HolMO(Li), HolMO(K), or HolMO(Cs)) was immersed in a 1 M HNO_3 solution (50 mL) for 2 days to obtain the extracted samples (HolMO(Li)-H, HolMO(K)-H, or HolMO(Cs)-H, respectively). The inserted and extracted samples were filtered, washed with water, and air-dried at 70 °C.

Chemical Analyses. The available oxygen of each sample was determined by the standard oxalic acid method as described before.¹⁷ The mean oxidation number (Z_{Mn}) of manganese was evaluated from the value of available oxygen. The lithium, potassium, cesium, and manganese contents were determined after dissolving the sample with a mixed solution of H_2SO_4 and H_2O_2 . Lithium, potassium, and cesium concentrations were determined by atomic absorption spectrometry. Manganese concentration was determined by absorption spectrometry at 523 nm after oxidizing Mn to Mn(VII) with $(\text{NH}_4)_2\text{S}_2\text{O}_8$.

Physical Analyses. An X-ray analysis was carried out using a Rigaku type RINT1200 X-ray diffractometer with a graphite monochromator. Any mechanical deviation of diffraction angles was corrected by scanning the whole angle range with silicon powder. Infrared spectra were obtained by the KBr method on a JEOL infrared spectrometer Model JTR-RFX3001. DTA-TG curves were obtained on a MAC Science thermal analyzer (System 001, TG-DTA 2000) at a heating rate of 10 °C/min.

pH Titration. A 0.1 g portion of HolMO was immersed in a mixed solution (10 mL) of MCl + MOH ($M = \text{Li}, \text{Na}, \text{K}, \text{Cs}, \text{or } (\text{CH}_3)_4\text{N}$) in varying ratios with intermittent shaking at 25 °C. The concentration of MCl was adjusted to 0.1 M. After the sample was shaken for 7 days, the pH of the supernatant solution was determined with a Horiba Model M8s pH meter.

Distribution Coefficient (K_d). K_d values of alkali and alkaline-earth metal ions were determined by the batch method. A 0.1 g portion of HolMO sample was immersed in

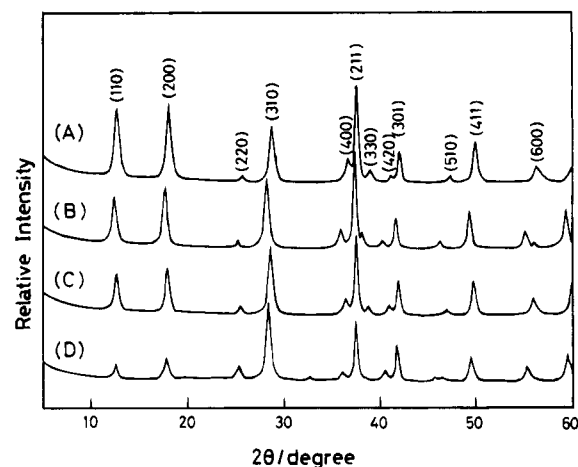


Figure 2. X-ray diffraction patterns of original and alkali metal ion inserted samples. From top: (A) HolMO; (B) HolMO(Li); (C) HolMO(K); (D) HolMO(Cs).

10 mL of a solution containing 10^{-3} M each of Li^+ , Na^+ , K^+ , Rb^+ , or Cs^+ , and a solution containing 5×10^{-4} M each of Mg^{2+} , Ca^{2+} , Sr^{2+} , and Ba^{2+} , respectively, at different pH values. The pH values were adjusted using HNO_3 solution. After attaining equilibrium (for 14 days), the metal ion concentration in the solutions was determined by atomic absorption spectrometry. The amount of metal ions adsorbed was calculated from the concentration relative to the initial concentration in the solution. The K_d value was calculated using the following equation:

$$K_d \text{ (mL/g)} = \frac{\text{metal ion uptake (mg/g of sample)}}{\text{metal ion concentration (mg/mL of solution)}}$$

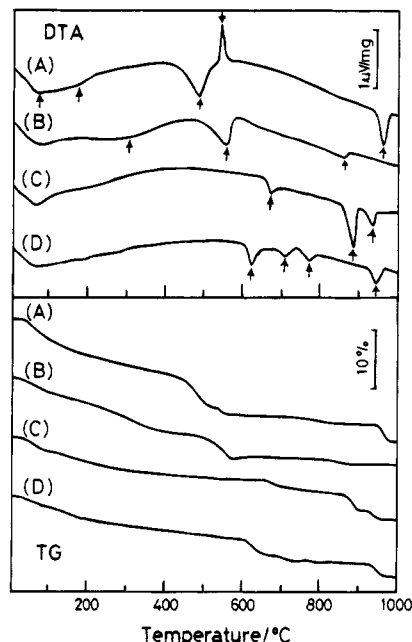
Results and Discussion

Characterization of Hollandite-Type Manganese Oxide. The X-ray diffraction pattern of HolMO is shown in Figure 2A. The X-ray diffraction data indicate that the crystal has a (2×2) tunnel structure which belongs to a body-centered tetragonal system (space group $I4/m$, Figure 1). The lattice parameters (Table 1) are in good agreement with those reported on $\alpha\text{-MnO}_2$ ($a = 9.78 \text{ \AA}$, $c = 2.86 \text{ \AA}$) prepared by treating Li_2MnO_3 with H_2SO_4 ⁹ and K^+ -extracted cryptomelane (CryMO, $a = 9.77 \text{ \AA}$, $b = 2.85 \text{ \AA}$).¹¹ Chemical analysis revealed that the HolMO contains only a small amount of Li^+ ($\text{Li/Mn} = 0.001$) and has the mean oxidation number of manganese (Z_{Mn}) of 4. The DTA curve shows an endothermic peak at 80 °C and a shoulder around 170 °C with weight losses (Figure 3A). The weight loss below 100 °C can be attributed to the evaporation of surface-adsorbed water, and the weight loss between 120 and 350 °C to the dehydration of the crystal water. The large endothermic peak at 480 °C with a weight loss corresponds to the decomposition of the hollandite framework associated with the release of oxygen, and the exothermic peak at 540 °C to the transformation to bixbyite (Mn_2O_3) associated with the release of a small amount of oxygen. The compositional formula of the HolMO can be written as $\text{MnO}_2 \cdot 0.21\text{H}_2\text{O}$, excluding the adsorbed water and ignoring a minor amount of Li^+ ; then the value 0.21 corresponds to the water content for crystal water (including lattice -OH groups).

Metal Ion Insertion in Aqueous Solution. The results of compositional analyses for the metal ions inserted samples (HolMO(Li), HolMO(K), and HolMO(Cs)) are given in Table 1. The alkali metal contents

Table 1. Compositional and Structural Parameters of Original and Alkali Metal Ion Inserted Samples, and Proportions of the Redox-Type and Ion-Exchange-Type Insertion Reactions^a

sample	Z_{Mn}	M/Mn ^a	crystal H ₂ O/Mn	lattice constant (Å)			insertion	
				<i>a</i>	<i>c</i>	<i>a/c</i>	red (%)	ion (%)
HolMO	4.00	0.001	0.21	9.79 ± 0.01	2.86 ± 0.01	3.42		
HolMO(Li)	3.91	0.270	0.34	9.99 ± 0.01	2.85 ± 0.01	3.50	33	67
HolMO(K)	3.94	0.195	0.18	9.87 ± 0.01	2.84 ± 0.01	3.47	31	69
HolMO(Cs)	3.97	0.123	0.18	9.96 ± 0.01	2.85 ± 0.01	3.49	24	76

^a M = Li, K, Cs.**Figure 3.** DTA (top) and TG (bottom) curves for original and alkali metal ion inserted samples. Symbols are the same as those in Figure 2.

increase in the order $Cs^+ < K^+ < Li^+$, in agreement with the decreasing order of the ionic radii. The crystal water content, which was evaluated from weight loss between 120 and 350 °C, decreases by the insertion of K^+ or Cs^+ . This suggests that there are some lattice -OH groups which are ion-exchangeable with metal ions in the crystal ($R-OH + M^+ \rightarrow R-OM + H^+$). The increase of the water content with Li^+ insertion suggests that Li^+ insertion accompanies water insertion.

The insertion reactions caused decreases in the Z_{Mn} value for all the metal ions studied (Table 1). The evolution of oxygen gas and the formation of a small amount of Mn(VII) were observed during the metal ion insertions. Kanzaki et al. have proposed the formation of small amount of Mn(VII) during the Li^+ insertion into spinel-type manganese oxide system as an evidence of redox-type insertion reaction.²⁰ The above facts suggest that a redox-type insertion reaction also occurs during the metal ion insertions into HolMO, in addition to the H^+/M^+ ion-exchange reaction.

Physical Properties of Alkali Metal Ion Inserted Samples. The X-ray diffraction patterns of HolMO(Li), HolMO(K), and HolMO(Cs) show that the hollandite structure was remained after the insertions (Figure 2). The insertions cause a small increase in the lattice constant *a* and a small decrease in lattice constant *c* (Table 1). This indicates that the metal ion insertion

reactions take place topotactically, involving a slight variation in the lattice constants. The marked change in the intensity of diffraction peaks for HolMO(Cs) may be due to the large X-ray scattering ability of inserted Cs^+ .

DTA-TG analyses were carried out for HolMO(Li), HolMO(K), and HolMO(Cs) samples (Figure 3). The DTA-TG curves for HolMO(Li) showed endothermic peaks around 80, 300, 560, and 850 °C, each with a weight loss (Figure 3B). These peaks correspond to the evaporation of surface adsorbed water, dissipation of the crystal water, the decomposition of Li^+ -form HolMO to $LiMn_2O_4$ spinel and bixbyite (Mn_2O_3) with the release of oxygen, and the transformation of bixbyite to hausmannite (Mn_3O_4) with the release of oxygen, respectively. In the DTA-TG curves for HolMO(K) (Figure 3C), endothermic peaks around 670, 880, and 930 °C with weight losses correspond to the transformation of K^+ -form HolMO to $K_2Mn_8O_{16}$ and bixbyite, $K_2Mn_8O_{16}$ to $K_2Mn_4O_8$ and bixbyite, and bixbyite to hausmannite, respectively.²¹ X-ray diffraction analysis shows that Cs^+ -form HolMO converts to $Cs_2Mn_8O_{16}$ and γ - Mn_2O_3 around 620 °C, and $Cs_2Mn_8O_{16}$ decomposes to bixbyite and an unknown compound around 780 °C. The endothermic peak around 710 °C corresponds to the transformation of γ - Mn_2O_3 to bixbyite. The above results indicate that the insertions of the metal ions cause the hollandite structure to stabilize thermally. K^+ is the most effective in stabilizing the hollandite structure, because the ion just fits the size of the (2 × 2) tunnel of the hollandite structure.

IR spectra of HolMO, HolMO(Li), and HolMO(K) are shown in Figure 4. In the spectrum of HolMO, there are two bands at 3240 and 3430 cm^{-1} for the stretching vibration of -OH groups. The band at 3240 cm^{-1} decreases in intensity with insertion of Li^+ and K^+ ions. The band at 3240 cm^{-1} can be assigned to a lattice -OH group; the proton (lattice proton) is ion exchangeable with the metal ion. The band at 3430 cm^{-1} can be assigned to the crystal water molecule which is located in the (2 × 2) tunnel site and the adsorbed water. These water molecules are ion-exchange inert. The increase in the intensity of the band at 3430 cm^{-1} with the Li^+ insertion suggests that the Li^+ insertion accompanies the insertion of water molecules into the (2 × 2) tunnel, in agreement with the results of the compositional analysis (Table 1).

Model for the Insertion Reaction. The above results show that metal ions can be inserted into HolMO by two different types of reactions: redox type and ion-exchange type. These reactions can be explained in terms of the structure of hollandite-type manganese oxide. The formula for an idealized hollandite-type

(20) Kanzaki, Y.; Taniguchi, A.; Abe, M. *J. Electrochem. Soc.* **1991**, *138*, 333.(21) Ohsato, H.; Sugimura, T. *J. Ceram. Soc. Jpn.* **1993**, *101*, 195.

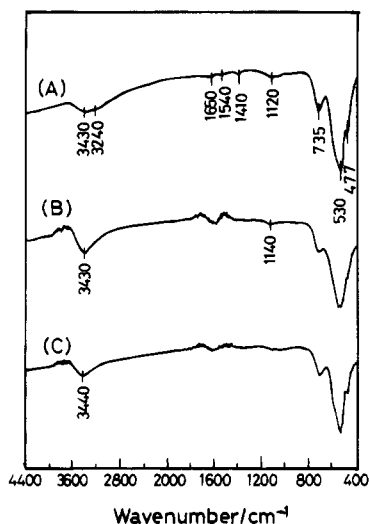
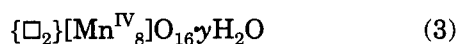
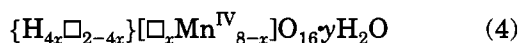


Figure 4. IR spectra of original and alkali metal ion inserted samples. Symbols are the same as those in Figure 2.

manganese oxide without any other cation in the (2×2) tunnel sites can be written as follows:

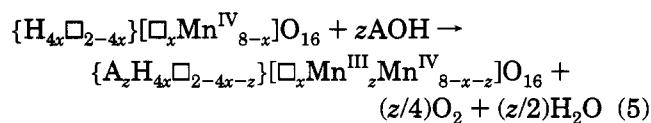


where $\{ \}$, $[]$, and \square are (2×2) tunnel sites, octahedral sites occupied by Mn, and vacant sites, respectively, and y is the number of crystal water molecules which are ion-exchange inert. A neutron diffraction study on the α - MnO_2 has indicated that there is a 9% defect in the Mn sites, and lattice protons may occupy the (2×2) tunnel sites.⁹ This shows the formation of defects in the octahedral Mn sites. The realistic formula for the present hollandite-type manganese oxide can be written with Mn defects as follows:



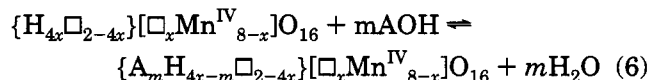
where x is the number of Mn defects, and $4x$ the number of ion-exchangeable lattice protons. The amount of protons is equal to 4 times the Mn defects by the condition of electroneutrality.

The metal ion insertion into the hollandite-type manganese oxide expressed by formula 3 is a redox-type reaction, because there are no protons that are exchangeable with metal ions. The redox-type insertion reaction can be described as



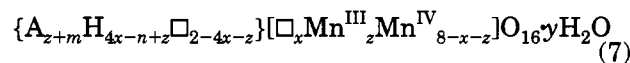
where the crystal water molecule ($y\text{H}_2\text{O}$) was omitted. The redox-type insertion reaction necessitates a reduction of Mn(IV) to Mn(III) as well as an oxidation of OH^- (or H_2O) to oxygen gas (and a small portion of disproportionation reaction of Mn(IV) to Mn(III) and Mn(VII)) at the solid surface, similar to the redox-type insertion of Li^+ into spinel-type manganese oxide.^{17,19,22} The diffusion of the metal ions through the (2×2) tunnel sites in the crystal accompanies a diffusion of electrons over the Mn atoms of the hollandite framework.

In the case of the hollandite-type manganese oxide expressed by formula 4, ion-exchange-type insertion reaction takes place with the lattice protons in the (2×2) tunnel sites, in addition to the redox-type insertion reaction. The ion-exchange-type reaction can be described as



In the ion-exchange-type reaction, the lattice protons are substituted by the metal ions.

X-ray diffraction study on the HolMO shows that there is only one solid phase in both the redox-type and ion-exchange-type reaction systems. Therefore, we think that these two types of reactions take place on a one-phase solid system, similar to the case of spinel-type manganese oxides.¹⁷ The metal ion inserted samples and HolMO can be expressed by a general formula:



where z is the number of alkali metal ions which are inserted by redox-type reaction and m those inserted by ion-exchange-type reaction ($0 \leq z + m \leq 2$).

Proportions of Redox-Type and Ion-Exchange-Type Insertion Reactions and Chemical Formulas for HolMO and Inserted Samples. The proportions of redox-type and ion-exchange-type insertions can be calculated using chemical analysis data as follows:

$$f_{\text{red}} = \Delta Z_{\text{Mn}} / (\Delta M / \text{Mn}) \quad (8)$$

$$f_{\text{ion}} = 1 - f_{\text{red}} \quad (9)$$

where f_{red} and f_{ion} are proportions of the redox-type and ion-exchange-type insertion reactions, respectively, ΔZ_{Mn} and $\Delta M / \text{Mn}$ differences of the mean oxidation number (Z_{Mn}) and the mole ratio of alkali metal ion to Mn before and after the alkali metal ion insertion. The equations are derived on the basis of the fact that the redox-type insertion necessitates a reduction of Mn(IV) to Mn(III). The proportions of the redox-type and the ion-exchange-type insertion reactions are estimated from the compositional data, as is given in Table 1. The proportions of redox-type and ion-exchange-type insertion reactions are about 30% and 70%, respectively, for the alkali metal ions studied here.

It is difficult to differentiate quantitatively the ion-exchangeable lattice $-\text{OH}$ group and the crystal water molecule in the HolMO. If the lattice proton content is assumed to be equal to the ion-exchange-type insertion capacity for Li^+ , the parameters x , n , z , and y in the general formula 7 can be evaluated from the chemical analysis data in Table 1 as follows:

$$(4x)/(8-x) = f_{\text{ion}}(\text{Li})(\text{Li}/\text{Mn})$$

$$x = \{8f_{\text{ion}}(\text{Li})(\text{Li}/\text{Mn})\} / \{4 + f_{\text{ion}}(\text{Li})(\text{Li}/\text{Mn})\} \quad (10)$$

$$n/(8-x) = (M/\text{Mn}), \quad n = (M/\text{Mn})(8-x) \quad (11)$$

(22) Ooi, K.; Miyai, Y.; Katoh, S.; Maeda, H.; Abe, M. *Langmuir* 1989, 5, 150.

Table 2. Formulas of Original and Alkali Metal Ion Inserted Samples

sample	x	n	z	y	formula
HolMO	0.34	0.00	0.00	0.93	$(\text{H}_{1.36}\square_{0.64})\{\square_{0.34}\text{Mn}^{\text{IV}}_{7.66}\}\text{O}_{16}\cdot 0.93\text{H}_2\text{O}$
HolMO(Li)	0.34	2.07	0.68	2.60	$(\text{Li}_{2.07})\{\square_{0.34}\text{Mn}^{\text{III}}_{0.68}\text{Mn}^{\text{IV}}_{6.98}\}\text{O}_{16}\cdot 2.60\text{H}_2\text{O}$
HolMO(K)	0.34	1.49	0.46	1.21	$(\text{K}_{1.49}\text{H}_{0.33}\square_{0.18})\{\square_{0.34}\text{Mn}^{\text{III}}_{0.46}\text{Mn}^{\text{IV}}_{7.20}\}\text{O}_{16}\cdot 1.21\text{H}_2\text{O}$
HolMO(Cs)	0.34	0.94	0.23	1.05	$(\text{Cs}_{0.94}\text{H}_{0.65}\square_{0.42})\{\square_{0.34}\text{Mn}^{\text{III}}_{0.23}\text{Mn}^{\text{IV}}_{7.43}\}\text{O}_{16}\cdot 1.05\text{H}_2\text{O}$

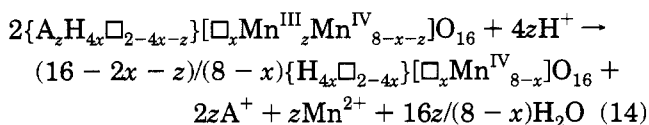
$$z/n = f_{\text{red}}, \quad z = n f_{\text{red}} \quad (12)$$

$$y = (\text{H}_2\text{O}/\text{Mn})(8 - x) - (4x + z - n)/2 \quad (13)$$

where $f_{\text{ion}}(\text{Li})$ (=0.67) and Li/Mn (=0.270) are the proportion of ion-exchange-type reaction and Li/Mn mole ratio for HolMO(Li) (Table 1), respectively. The formulas and the parameters x , n , z , and y for HolMO and the metal ion inserted samples are given in Table 2. The manganese site occupancy for HolMO is estimated as about 0.96, which is a little larger than that for the α - MnO_2 (0.91).⁹

Extraction of Alkali Metal Ions from the Metal Ion Inserted Samples with Acid Treatment. Extraction reactions of alkali metal ions were investigated on the alkali metal ion inserted samples (HolMO(Li), HolMO(K), and HolMO(Cs)) using a 1 M HNO_3 solution. The acid-treatment extracts 96% of Li^+ , 48% of K^+ , and 40% of Cs^+ from the metal ion inserted samples (Table 3). This suggests that Li^+ with a small ionic radius can move easily in the (2×2) tunnel, but K^+ and Cs^+ with large ionic radii are tightly fixed on the (2×2) tunnel sites. The X-ray diffraction patterns of the acid-treated samples showed that the hollandite structures remained after the extractions of the alkali metal ions, indicating that the extraction reactions proceed topotactically. The extraction of the alkali metal ions was attended by the dissolution of a small amount of Mn^{2+} into the solution (Table 3).

Ion-exchange-type reactions also take place in the extraction step. The ion-exchange-type extraction reaction can be expressed by eq 6. On the other hand, the dissolution of Mn^{2+} supports the presence of redox-type reaction. Hunter has proposed a redox-type reaction for the Li^+ extraction from LiMn_2O_4 spinel;²³ the reaction has been characterized by the dissolution of Mn^{2+} . The dissolution of Mn^{2+} is due to a surface disproportionation reaction of Mn(III) ($\text{Mn}^{\text{III}} \rightarrow 1/2\text{Mn}^{\text{IV}} + 1/2\text{Mn}^{\text{II}}$). Similar to the case of LiMn_2O_4 spinel, the redox-type extraction of alkali metal ions can be written for hollandite-type manganese oxides as follows:



The extraction of alkali metal ions accompanies the disproportionation of Mn(III) to Mn(IV) and Mn(II). The Mn(IV) remains in the solid phase, and Mn(II) dissolves into the solution phase.

The proportion of the redox-type extraction can be estimated from the amount of Mn dissolved as follows:

$$f_{\text{red}} = 2n_{\text{Mn}}/n_{\text{A}} \quad (15)$$

where f_{red} , n_{Mn} , and n_{A} are the fraction of redox-type extraction reaction, mole of dissolved Mn^{2+} , and mole

Table 3. Amounts of Alkali Metal Ions Extracted and Manganese Dissolved by Acid Treatment and Proportions of Redox-Type and Ion-Exchange-Type Extraction Reactions^a

sample	M extracted (%)	Mn dissolved (%)	extraction	
			red (%)	ion (%)
HolMO(Li)-H	96	4.2	34	66
HolMO(K)-H	48	0.62	14	86
HolMO(Cs)-H	40	0.87	33	67

^a M = Li, K, Cs.

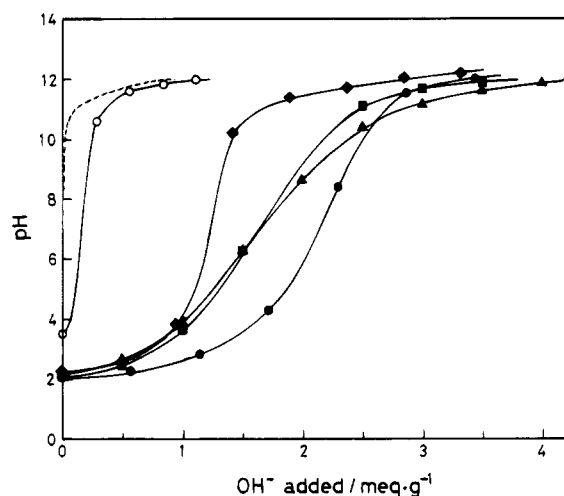


Figure 5. pH titration curves for HolMO: sample, 0.1 g; solution, 0.1 M $\text{MCl} + \text{MOH}$ ($\text{M} = \text{Li}$ (\blacktriangle), Na (\blacksquare), K (\bullet), Cs (\blacklozenge), or $(\text{CH}_3)_4\text{N}$ (\circ)); total volume of solution, 10 mL; temperature, 20 °C; (---) blank titration.

of extracted alkali metal ions, respectively. The residual fraction can be regarded as an ion-exchange-type extraction reaction. The fractions of the ion-exchange-type extraction reaction are higher than those of the redox-type extraction reaction (Table 3). The fractions of the redox-type and ion-exchange-type reactions for Li^+ and Cs^+ extractions are close to those of the insertion reactions (Tables 1 and 3). The lower fraction of the redox-type reaction for K^+ extraction than those of the insertion reaction suggests that K^+ is extracted more easily by the ion-exchange-type reaction than by the redox-type reaction.

The redox-type and ion-exchange-type extraction reactions can be regarded as a one-phase solid solution reaction similar to the spinel-type manganese oxide system.¹⁷ The metal ions migrate to the surface of the crystal and are transported into the solution phase. The dissolution of Mn according to reaction 14 proceeds at the crystal surface, owing to the free movement of electrons.

pH Titration. The pH titration curves of HolMO in (0.1 M $\text{ACl} + \text{AOH}$, $\text{A} = \text{Li}$, Na , K , Cs , and $(\text{CH}_3)_4\text{N}$) solutions are shown in Figure 5. The HolMO shows a monobasic behavior toward all these alkali metal ions and $(\text{CH}_3)_4\text{N}^+$. The formations of Mn^{VII} were observed in the solutions of alkali metal ions when $\text{pH} > 11$. This suggests that redox-type adsorption occurs at a high pH

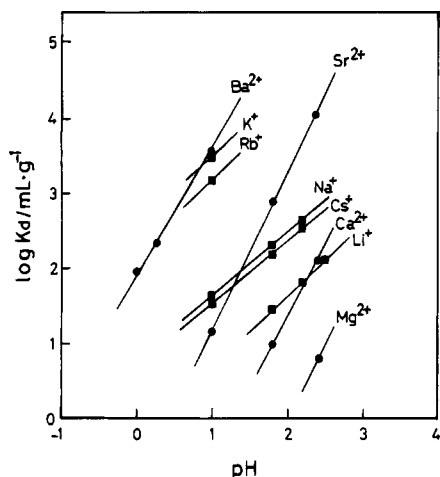


Figure 6. Plots of $\log K_d$ against the solution pH: (■) alkali; (●) alkaline earth metal ions.

range. The present pH titration curves are different from those in the case¹² of CryMO where dibasic behavior toward Li^+ , Na^+ , K^+ , and Rb^+ , and monobasic behavior toward Cs^+ have been observed. HolMO shows larger apparent capacities for Li^+ , Na^+ , and K^+ than CryMO, and almost the same apparent capacity for Cs^+ as CryMO.

The apparent capacity (about 0.2 mmol/g) for $(\text{CH}_3)_4\text{N}^+$ is remarkably smaller than those for the alkali metal ions over the pH range studied. This is due to the steric effect of the (2×2) tunnel site, since $(\text{CH}_3)_4\text{N}^+$ ions cannot enter the (2×2) tunnel sites, owing to their too large ionic radii (3.5 Å).²⁴ These ions exchange with the protons of surface $-\text{OH}$ group alone. However, the alkali metal ions not only can exchange with the protons of surface $-\text{OH}$ group but also can enter the (2×2) tunnel sites after dehydration (or partial dehydration). The apparent capacity for the alkali metal ion increases in the order $\text{Cs}^+ < \text{Li}^+$, $\text{Na}^+ < \text{K}^+$ at $\text{pH} < 10$, showing a strong affinity toward K^+ . It is well-known that the size of K^+ fits the (2×2) tunnel site. The affinity sequence changes to $\text{Cs}^+ < \text{K}^+ < \text{Na}^+ < \text{Li}^+$ at $\text{pH} > 10$; the sequence is in agreement with the decreasing order of effective ionic radius of metal ions. Larger cations suffer a larger steric interaction with each other in a state of high metal ion loading.

Selectivity of Alkali and Alkaline Earth Metal Ions. The equilibrium K_d values of alkali and alkaline earth metal ions on HolMO are plotted as a function of solution pH in Figure 6. The logarithms of the K_d values

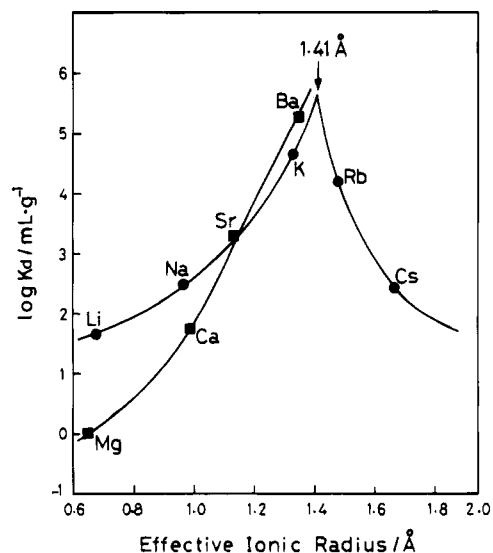


Figure 7. Distribution coefficients (K_d) of alkali and alkaline earth metal ions on the HolMO at pH 2 as a function of effective ionic radius.

increase linearly with increasing pH in the pH range studied. The slopes of $d \log K_d / d \text{pH}$ are close to 1 for alkali metal ions and close to 2 for alkaline earth metal ions. The selectivity sequence is $\text{Li}^+ < \text{Cs}^+$, $\text{Na}^+ \ll \text{Rb}^+ < \text{K}^+$ for alkali metal ions and $\text{Mg}^{2+} < \text{Ca}^{2+} < \text{Sr}^{2+} < \text{Ba}^{2+}$ for alkaline earth metal ions over the pH range studied. A characteristic feature is that HolMO has extremely high selectivities for K^+ , Rb^+ , and Ba^{2+} , similar to the case of the CryMO.¹¹ This feature can be explained on the basis of the ion-sieve effect of the (2×2) tunnel sites in the hollandite lattice. A plot of $\log K_d$ against the effective ionic radius of the metal ion²⁵ indicates that HolMO shows the highest K_d value at 1.41 Å (Figure 7). This result suggests that the pore size of HolMO is most suitable for fixing an ion with an effective ionic radius of 1.41 Å. On the basis of the present results, we define the radius as an effective pore radius for the ion-sieve-type adsorbent.

Conclusions

Alkali metal ions can be inserted/extracted topotactically into/from the HolMO. The insertion/extraction reactions proceed by two types of mechanisms: a redox-type and an ion-exchange-type. The HolMO shows an ion-sieve effect for the adsorption of metal cation ions. The effective pore radius of HolMO is 1.41 Å.

CM940343U

(24) Robinson, R. A.; Stokes, R. H. *Electrolyte Solutions*; Academic Press: New York, 1959.

(25) Shannon, R. D.; Prewitt, C. T. *Acta Crystallogr.* **1969**, *B25*, 925.